



Natural Resources
Canada

Ressources naturelles
Canada

**GEOLOGICAL SURVEY OF CANADA
OPEN FILE 8224**

**Historical fluctuations of lake shorelines based on geomorphological
analysis in the vicinity of Rankin Inlet, Nunavut**

O. Bellehumeur-Génier, G.A. Oldenborger, and A-M. LeBlanc

2017



Canada



GEOLOGICAL SURVEY OF CANADA OPEN FILE 8224

Historical fluctuations of lake shorelines based on geomorphological analysis in the vicinity of Rankin Inlet, Nunavut

O. Bellehumeur-Génier, G.A. Oldenborger, and A.-M. LeBlanc

2017

© Her Majesty the Queen in Right of Canada, as represented by the Minister of Natural Resources, 2017

Information contained in this publication or product may be reproduced, in part or in whole, and by any means, for personal or public non-commercial purposes, without charge or further permission, unless otherwise specified.

You are asked to:

- exercise due diligence in ensuring the accuracy of the materials reproduced;
- indicate the complete title of the materials reproduced, and the name of the author organization; and
- indicate that the reproduction is a copy of an official work that is published by Natural Resources Canada (NRCan) and that the reproduction has not been produced in affiliation with, or with the endorsement of, NRCan.

Commercial reproduction and distribution is prohibited except with written permission from NRCan. For more information, contact NRCan at nrcan.copyrightdroitdauteur.nrcan@canada.ca.

<https://doi.org/10.4095/301750>

This publication is available for free download through GEOSCAN (<http://geoscan.nrcan.gc.ca/>).

Recommended citation

Bellehumeur-Génier, O., Oldenborger, G.A., and LeBlanc, A.-M., 2017. Historical fluctuations of lake shorelines based on geomorphological analysis in the vicinity of Rankin Inlet, Nunavut; Geological Survey of Canada, Open File 8224, 1 .zip file. <https://doi.org/10.4095/301750>

ABSTRACT

The purpose of this Open File is to provide information derived from the analysis of lake shorelines in the vicinity of Rankin Inlet, Nunavut. The analysis focused on three areas of interest located north of Rankin Inlet, with different surficial material mosaics. A total of 220 lakes were digitized from air photos and satellite imagery using a geographical information system (GIS) for the period 1954 to 2014. Lake surface areas were computed using the digitized polygons. A visual assessment of the geomorphological dynamics of individual lakes was undertaken to differentiate normal shoreline behavior from that potentially associated with thermokarst. Results showed that lakes in the areas of interest have experienced significant shoreline fluctuation as part of normal lake behavior. Despite the high degree of normal shoreline variability, the geomorphological analysis revealed that certain lakes demonstrated abnormal increases or decreases in area, along with localized shoreline dynamics.

TABLE OF CONTENTS

ABSTRACT.....	iii
TABLE OF CONTENTS.....	iv
INTRODUCTION	1
STUDY AREA	1
Study sites	3
METHODOLOGY	4
RESULTS	7
Area of Interest 1	7
Area of Interest 2	7
Area of Interest 3	8
LIMITATIONS.....	8
CONCLUSIONS.....	9
ACKNOWLEDGEMENTS	9
REFERENCES	9

INTRODUCTION

Understanding permafrost characteristics and processes is of foremost importance in the context of a warming climate. For the western coast of Hudson Bay in the Kivalliq Region of Nunavut, the mean annual air temperature (MAAT) has increased by 2°C since 1981 (Environment Canada, 2016). At the same time, the region is undergoing significant infrastructure development associated with natural resources and community sustainability. Climate change resilience planning of communities and industries relies on geoscience information on permafrost and ground ice conditions. However, there is limited historical or contemporary permafrost data available along the western coast of Hudson Bay. This Open File summarizes observations of lake shoreline dynamics near Rankin Inlet as an initial assessment of thermokarst potential for the region.

Thermokarst is a process that alters the land surface, creating characteristic landforms that result from the melting of massive ice or the thawing of ice-rich permafrost (van Everdingen, 1998; Kokelj and Jorgenson, 2013). Thermokarst lakes are characteristic landforms of permafrost terrain that occupy closed depressions formed by the settlement of ice-rich ground. Existing lakes (of thermokarst origin or not) can also evolve through thermokarst processes such as active-layer detachment, retrogressive thaw slumps, or ice wedge degradation resulting in changes to the shoreline morphology, lake expansion, or lake drainage.

STUDY AREA

Rankin Inlet is a hamlet located on the western coast of Hudson Bay in the administrative region of the Kivalliq, Nunavut (Figure 1). Rankin Inlet is 200 km north of the hamlet of Arviat and 90 km south of Chesterfield Inlet (Figure 1). The region was covered by the Laurentide Ice Sheet and the Keewatin Dome during the Wisconsin Glaciation and was greatly influenced by the

Keewatin Ice Divide (Shilts et al., 1979). Deglaciation of the region was initiated around 11 ka; by 8 ka the ice sheet limit was near Baker Lake, and the entire region was free of ice by 5 ka (Shilts et al., 1979; Hivon and Segó, 1993). The postglacial Tyrrell Sea extended as much as 150 km inland from the current coastline over the isostatically depressed land surface, reaching a maximum elevation of approximately 170 m above present sea level (Dyke, 2004; Randour et al., 2016). In Arviat, the crustal uplift is estimated to be around 9.3 ± 1.5 mm/yr (Simon et al., 2014) and the relative sea level is decreasing at approximately 6.4 mm/year as a result of crustal uplift exceeding sea level rise (Allard et al., 2014). The surficial geology of the immediate area surrounding Rankin Inlet consists of glacial, marine, and glaciofluvial deposits with numerous bedrock outcrops (McMartin, 2002). The geomorphological environment surrounding Rankin Inlet includes eskers, ice-wedge polygons, mudboils, active-layer detachments, and gelifluction lobes (McMartin, 2002; LeBlanc et al., 2016).

Rankin Inlet is located within the continuous permafrost zone (> 90% of the land underlain by permafrost) and the area is described as having low ground ice potential (< 10%) with the sparse occurrence of ice-wedge polygons (Heginbottom et al., 1995). Active-layer thickness in the vicinity of Rankin Inlet ranges from 30 cm in till/marine sediments to 400 cm in bedrock and permafrost thickness varies from 300 to 500 m thick (Brown, 1963; Brown, 1978; Smith et al., 2005). Mean annual ground temperature (MAGT) has been reported to range from -6.4 to -7.9°C at 4 to 14 m depth (Brown, 1978). Permafrost along the western coast of Hudson Bay may exhibit high salinity due to post-glacial inundation (Hivon and Segó, 1995). The snow cover is generally windblown with thicknesses varying from 25 to 45 cm in natural tundra-dominated terrain (Brown, 1978; Smith et al., 2005; Throop et al., 2012).

The average MAAT recorded at Rankin Inlet Airport from 1982 to 2012 is 10.3°C (Environment Canada, 2016). During the same time period, the MAAT has increased at an average rate of 0.068°C/year, corresponding to an overall increase of approximately 2°C (LeBlanc et al., 2016). Recent studies suggest significant changes to permafrost distribution and characteristics in this region as a result of projected increases in MAAT and decrease in sea ice cover on Hudson Bay (Gagnon and Gough, 2005a; Gagnon and Gough, 2005b; Zhang, 2013; Tam, 2014).

Study sites

Three areas of interest (AOI) were selected in the vicinity of Rankin Inlet based on the potential for thermokarst and air photo and satellite imagery coverage in space and time. For the purposes of site selection, the potential for thermokarst was qualitatively determined based on the surficial geology (high occurrence of marine sediments), the presence of ice-rich periglacial landforms (ice wedges, gelifluction lobes), and lake density.

Area of Interest 1 (AOI 1) is located approximately 12 km northwest of Rankin Inlet and 2 km west of the Iqalugaarjuup Nunanga Territorial Park in natural terrain unaltered by anthropogenic influence (Figures 1 and 2, Table 1). The surficial geology consists mainly of glacial deposits dominated by till veneer (Tv), till blanket (Tb), and undifferentiated till and marine sediments (T.M) (McMartin, 2002; GSC, in press). Present to lesser extent are ridge moraine (Tr), hummocky till (Th), nearshore marine sediments (Mn), and beach sediments (Mr) (McMartin, 2002; GSC, in press). Ice-wedge polygons are found predominantly in units containing some marine sediment (T.M, Mn, and Mr), drumlins are mapped on the till units (Tb and Tv) often associated with gelifluction lobes, DeGeer moraines are mapped on the Tv unit, and numerous hummocks and rigged moraines are mapped on the Th unit (McMartin, 2002; GSC, in press).

Area of Interest 2 (AOI 2) is located approximately 10 km northwest of Rankin Inlet in the Iqalugaarjuup Nunanga Territorial Park (Figures 1 and 3). AOI 2 was intersected by the territorial park access road, which was constructed on an esker in the 1970s and further developed in the following years. AOI 2 surficial geology is dominated by subaqueous outwash fan sediments (GFf2), hummocky sediments (GFh), ice-contact sediments (GFc), alluvial sediments (A), and undifferentiated alluvial and marine sediments (A.M) (McMartin, 2002; GSC, in press). Glacial sediments T.M, Th, Tr and Tb are also found in AOI 2. Patches of Mr are found in the southern portion of AOI 2 and undifferentiated bedrock outcrops (R) are mapped in the west central sector (McMartin, 2002; GSC, in press). The main landforms observable in AOI 2 are ice-wedge polygons found in glacial, glaciofluvial, and marine deposits, kettle lakes adjacent to the esker, and the esker itself (McMartin, 2002; GSC, in press).

Area of Interest 3 (AOI 3) is located 10 km north of Rankin Inlet (Figures 1 and 4). The vast majority of AOI 3 is in natural undisturbed terrain, although a small portion is crossed by the access road for Agnico Eagle Mines Limited's advanced-stage Meliadine gold project constructed in the early 2000s. The surficial geology consists of glacial (T.M, Tb, and Tv), glaciofluvial (GFc and GFh), alluvial (A.M), and organic (O) sediments (McMartin, 2002; GSC, in press). Numerous bedrock outcrops (R) are found in this area (McMartin, 2002; GSC, in press). An esker traverses AOI 3 on the GFc unit and ice-wedge polygons are wide spread (McMartin, 2002; GSC, in press). Kettle lakes are mapped in the northern sector and DeGeer moraines are mapped perpendicular to the esker in glaciofluvial sediments (McMartin, 2002; GSC, in press).

METHODOLOGY

The methodological approach was primarily based on visual geomorphological analysis of historical air photos and satellite imagery to establish temporal lake shoreline evolution. The

geomorphological analysis was combined with climate and surficial geology data and validated by limited field observations.

For AOI 1, a total of 51 lakes and ponds were digitized for analysis. Air photos from 1954, 1969, 1986 and 1992 were used in combination with satellite imagery from 2005 and 2014. For AOI 2, a total of 83 lakes were digitized for analysis. Air photos from 1954, 1965, 1969, 1986 and 1992 were used, with satellite imagery from 2005, 2012 and 2014. For AOI 3, a total of 88 lakes and ponds were digitized for analysis. Air photos from 1954, 1961, 1965, 1969 and 1975 were used in combination with satellite imagery from 2005.

For each AOI, the shorelines of lakes and ponds were manually digitized as polygons for each year of available data. The air photos retained for analysis were from 1954, 1961, 1965, 1969, 1972, 1975, 1976, 1986, and 1992. Selected air photos were all taken during summer months (July and August) in order to ensure consistency in ground conditions and the degree of thaw. The satellite imagery used consisted of Worldview 2 images from 2012 and 2014, and satellite imagery available from Google Earth Pro in 2005. Air photos were orthorectified on the NTS map prior to analysis with a root-mean-square error (RMSE) averaging of 0.5 m (Table 2). Lake shorelines were digitized in ESRI ArcGIS 10.2.2 using the editor tool for each year where data were available and areas were calculated based on the digitized polygons. Some lake shorelines were difficult to assess and subject to operator judgement due to image clarity and marshy conditions. Therefore, three independent operators repeated the digitization of 48 lakes from AOI 1, representing about 23% of the sample for one year (Paul et al., 2013; Way et al., 2014). This analysis provides an estimate of the error associated with the digitized areas for the selected lakes (Table 3). The average digitization error for all the selected lakes is 9% of lake area. Combining average operator

error with the orthorectification error of 0.5 m, the total lake area error is approximated as $\Delta A = 0.09A + (\pi A)^{1/2}$ or $\Delta A/A = 0.09 + (\pi/A)^{1/2}$ for a circular lake, which increases for small lakes.

For each AOI lake, the presence or absence of thermokarst was assessed using visual observations of shoreline morphology and evolution through time. For each lake, each year's imagery was assessed both individually, and as part of the time series to distinguish normal shoreline behavior from potential thermokarst processes. In each AOI, the lakes exhibited an annual oscillation of their shoreline limit due to natural hydrological cycles. Warming of air temperature along the western coast of Hudson Bay was most pronounced from 1990 to the early 2000s (LeBlanc et al., 2016). Therefore, particular attention was made to identifying significant abnormal geomorphological changes evident from 2005 and 2014. Shoreline behavior was categorized as stable, expanding or draining, along with some description of the localized or generalized nature of shoreline evolution and the surficial geology. Before classifying lakes, the complete record was visually analyzed and normal lake behavior was established by observing shoreline maximum-minimum extent and morphology. Stable lakes were characterized by normal shoreline fluctuation over time with varying amplitude and a lack in abnormal change of their shoreline, which differed greatly from previous observations. In contrast, expanding or draining lakes were defined according to observations of shoreline morphological evolution that visually differed greatly from previous fluctuations and/or amplitude of shoreline oscillation in previous years. Following this approach, lakes could have more than one count of surficial material associated with lake shoreline change because of the complex distribution of the surficial geology in the area, such that a lake may overly more than one surficial unit. A count is then attributed to each surficial unit present in an expansion/drainage affected lake.

RESULTS

Individual lake surface area time series data, computed using the digitized polygons, are presented in Appendix A. The results of the geomorphological analysis of lakes through time are presented in Appendix B and will be discussed in this section. The surface area data (Appendix A) are not used in the current analysis, but may provide insight for future studies.

Area of Interest 1

Out of the 55 lakes and ponds digitized in AOI 1, 11 have experienced expansion, 5 have seen a significant decrease in area, and 35 are considered stable. Lake expansion was first observed in 2005 and commonly progressed into 2012–14 for all lakes affected by this phenomenon (Appendix B). For large lakes, much of the expansion was localized, meaning that the increase in area was concentrated in a particular sector of the lake while the remaining shoreline of the lake was largely unchanged. Analyses focused on lake area alone (Appendix A) may be insensitive to this form of expansion which constitutes a relatively small portion of the total lake area. Of the 11 lakes exhibiting expansion, 10 counts were in glacial sediments with T.M being the dominant unit (7 counts) and Tv being of secondary importance (5 counts) (Figure 5 A). Marine sediments are associated with a smaller proportion of expansion with 3 counts in Mr and 2 counts in Mn (Figure 5 A). Lake drainage was most pronounced in 2014 for all drainage observations. Of the lakes with a decrease in area, 2 counts were in T.M, 2 counts were in Mr, 1 count in R.Mr units, and 1 count in Mn (Figure 5 A).

Area of Interest 2

In AOI 2, 83 lakes and ponds were digitized, of which 11 exhibited abnormal shoreline dynamics (Appendix B). Of these 11 lakes, drainage was the dominant process (9 out of 11 lakes). For the majority of lakes that exhibited drainage, changes were first observed in 2005. These

changes were concentrated in the Gfh.T unit (5 counts), followed by the GFf2 unit (3 counts), and the Tr and A units (1 count each) (Figure 5 B). Three of the drained lakes were found adjacent to the territorial park access road. Lake expansion occurred only for two large lakes in units T.M, Tb, Tv, and A (Figure 5 B). Expansion was observed in 2005 with continued growth in 2014.

Area of Interest 3

In AOI 3, 88 lakes and ponds were digitized, of which 11 lakes exhibited expansion or drainage (Appendix B). Lake expansion occurred most often in T.M (6 counts) and GFf2 (3 counts), the dominant surficial units in AOI 3, and in Tv and Mn (1 count each) (Figure 5 C). With the exception of lakes 86 and 90 that were covered by WorldView 2014 imagery, the most recent imagery for AOI 3 was 2005. Lakes 86 and 90 also differed from the rest of the sample due to their proximity to the recently-built access road for Agnico Eagle Mines Limited's Meliadine gold project. As such, lakes 86 and 90 may be subject to anthropogenic effects in addition to natural permafrost processes.

LIMITATIONS

We focused on 2D analysis of lake shorelines, which does not necessarily capture all possible changes related to thermokarst-affected lakes. Vertical lake expansion and/or drainage have been shown to affect high latitude lakes in North America and Siberia (Langer et al., 2016; MacDonald et al., 2016). Therefore, thermokarst processes that manifest as vertical changes in lake levels will go undetected by our methodology and result in an underestimation of thermokarst occurrence. This limitation might be addressed by incorporation of high resolution multispectral satellite imagery of lake depth.

CONCLUSIONS

A survey of lake shoreline dynamics from 1954 to 2014 was undertaken using remotely sensed data. The survey provided information on lake area and shoreline morphology for each year with available data. Geomorphological analysis of shoreline evolution through time was used to classify lakes as stable, expanding, or draining. Further analysis of the information is needed to establish the nature of the processes responsible for the observed lake behavior, but preliminary observations show a potential for occurrence of thermokarst affected lakes in the vicinity of Rankin Inlet from 2005 to 2014.

ACKNOWLEDGEMENTS

The authors thank D. Kerr of the Geological Survey of Canada, who provided up-to-date surficial geology maps for the region. This research is a partnership between the Geological Survey of Canada and the Canada Nunavut Geoscience Office. The authors also want to acknowledge critical reviewer Wendy Sladen for her constructive comments on the report. Worldview 2 images, copyright DigitalGlobe Inc., all rights reserved. Google Earth Pro images, copyright 2005 DigitalGlobe, copyright 2005 Google.

REFERENCES

- Allard, M., Manson, G.K. and Mate, D.J. 2014: Reconnaissance assessment of landscape hazards and potential impacts of future climate change in Whale Cove, southern Nunavut; *in* Summary of Activities 2013, Canada-Nunavut Geoscience Office, p. 171–182.
- Brown, R.J.E. 1963: Relation between mean annual air and ground temperatures in the permafrost region of Canada; *in* Proceedings of the Permafrost International Conference, Lafayette, Indiana, November 1963, p. 241–246.

- Brown, R.J.E. 1978: Influence of climate and terrain on ground temperatures in the continuous permafrost zone of northern Manitoba and Keewatin district, Canada; *in* Proceedings of the Third International Conference on Permafrost, Edmonton, Alberta, July 1978, v. 1, p. 15–21.
- Cocking, R.B., Deblonde, C., Kerr, D.E., Campbell, J.E. , Eagles, S., Everett, D., Huntley, D.H., Inglis, E., Lavolette, A., Parent, M., Plouffe, A., Robertson, L., St-Onge, D.A. and Weatherston, A. 2015: Surficial Data Model, version 2.1.0: revisions to the science language of the integrated Geological Survey of Canada data model for surficial geology maps; Geological Survey of Canada, Open File 7741, 276 .
- Dyke, A.S. 2004: An outline of North American deglaciation with emphasis on central and northern Canada; *Developments in Quaternary Science*, v. 2, p. 373–424.
- Environment** Canada 2016: Canadian climate normals; Environment Canada, <http://climate.weather.gc.ca/climate_normals/index_e.html> [August 2015].
- Gagnon, A. and Gough, W.A. 2005a: Trends in the dates of ice freeze-up and breakup over Hudson Bay, Canada; *Arctic*, v. 58, no. 4, p. 370–382.
- Gagnon, A. and Gough, W.A. 2005b: Climate change scenarios for the Hudson Bay region: an intermodel comparison; *Climate Change*, v. 69, p. 269–297.
- Geological Survey of Canada, in press : Surficial geology, Rankin Inlet, Nunavut, NTS 55-K/16; Geological Survey of Canada, Canadian Geoscience Map 68 (preliminary, Surficial Data Model v2.1 conversion of Open File 4116), scale 1:50 000.
- Heginbottom, J.A., Dubreuil, M.A. and Harker, P.T. 1995: Canada: Permafrost; *National Atlas of Canada*, Fifth Edition, Natural Resources Canada, MCR 4177.

- Hivon, E.G. and Segó, D.C. 1993: Distribution of saline permafrost in the Northwest Territories, Canada; *Canadian Geotechnical Journal*, v. 30, p. 506–514.
- Hivon, E.G. and Segó, D.C. 1995: Strength of frozen saline soils; *Canadian Geotechnical Journal*, v. 32, p. 336–354.
- Kokelj S.V. and Jorgenson, M.T. 2013: Advances in thermokarst research; *Permafrost and Periglacial Processes*, v. 24, p. 108–119.
- Langer, M., Westermann, S., Bolke, J., Kirillin, G., Grosse, G., Peng, S. and Krinner, G. 2016: Rapid degradation of permafrost underneath waterbodies in tundra landscapes – Toward a representation of thermokarst in land surface models; *Journal of Geophysical Research: Earth Surface*, 121, doi:10.1002/2016JF003956.
- Leblanc, A.M., Bellehumeur-Génier, O., Oldenborger, G. and Tremblay, T. 2016: Understanding permafrost conditions through integration of local and traditional observations with geoscience data in the vicinity of Rankin Inlet, western Hudson Bay, Nunavut; *in Summary of Activities 2016, Canada-Nunavut Geoscience Office*, p. 75-88.
- MacDonald, L.A., Turner, K.W., Balasubramaniam, A.M., Wolfe, B.B., Hall, R.I. and Sweetman, J.N. 2012: Tracking hydrological responses of a thermokarst lake in the Old Crow Flats (Yukon Territory, Canada) to recent climate variability using aerial photographs and paleolimnological methods; *Hydrological Processes*, v.26, p.117-129.
- McMartin, I. 2002: Surficial geology, Rankin Inlet, Nunavut; *Geological Survey of Canada, Open File 4116*, scale 1:50 000, doi: 10.4095/213219.
- Paul, F., Barrand, N.E., Baumann, S., Berthier, E., Bolch, T., Casey, K., Frey, H., Joshi, S.P., Konovalov, V., Le Bris, R., Mölg, N., Nosenko, G., Nuth, C., Pope, A., Racoviteanu, A.,

- Rastner, P., Raup, B., Scharrer, K., Steffen, S. and Winsvold, S. 2013: On the accuracy of glacier outlines derived from remote-sensing data; *Annals of Glaciology*, v. 54(63), doi: 10.3189/2013AoG63A296.
- Randour, I., McMartin, I. and Roy, M. 2016: Study of the postglacial marine limit between Wager Bay and Chesterfield Inlet, western Hudson Bay, Nunavut; *in* Summary of Activities 2016, Canada-Nunavut Geoscience Office, p. 51-60.
- Simon, K.M., James, T.S., Henton, J.A. and Dyke, A.S. 2016: A glacial isostatic adjustment of model for the central and northern Laurentide Ice Sheet based on relative sea level and GPS measurements; *Geophysical Journal International*, v.205, p. 1618-1636.
- Shilts, W.W., Cunningham, C.M. and Kaszycki., C.A. 1979: Keewatin Ice Sheet – Re-evaluation of the traditional concept of the Laurentide Ice Sheet; *Geology*, v.7, p. 537-541.
- Short, N., LeBlanc, A.-M. and Bellehumeur-Génier, O., 2016: Seasonal surface displacement derived from DInSAR, Rankin Inlet, Nunavut; Geological Survey of Canada, Canadian Geoscience Map 291 (preliminary), scale 1:50 000, doi:10.4095/298815
- Smith, S.L., Burgess, M.M., Riseborough, D. and Nixon, F.M. 2005a: Recent trends from Canadian permafrost thermal monitoring network sites; *Permafrost and Periglacial Processes*, v. 16, p. 19–30.
- Tam, A. 2014: The impacts of climate change on potential permafrost distributions from the subarctic to the high arctic regions in Canada; Ph.D. thesis, University of Toronto, Toronto, Ontario, 168 p., URL <<http://hdl.handle.net/1807/68103>> [November 2015].

Throop, J., Lewkowicz, A.G. and Smith, S.L. 2012: Climate and ground temperature relations at sites across the continuous and discontinuous permafrost zones, northern Canada; Canadian Journal of Earth Sciences, v. 49, p. 865–876.

van Everdingen, R.O. (ed.) 2005 (revised edition): Multi-language glossary of permafrost and related ground-ice terms; International Permafrost Association, , <http://globalcryospherewatch.org/reference/glossary_docs/Glossary_of_Permafrost_and_Ground-Ice_IPA_2005.pdf>.

Way, R.G., Bell, T. and Barrand, N.E. 2014: An inventory and topographic analysis of glaciers in the Torngat Mountains, northern Labrador, Canada; Journal of Glaciology, v.60, no. 223, doi: 10.3189/2014JoG13J195.

Zhang, Y. 2013: Spatio-temporal features of permafrost thaw projected from long-term high-resolution modeling for a region in the Hudson Bay Lowlands in Canada; Journal of Geophysical Research, v. 118, p. 542–552.

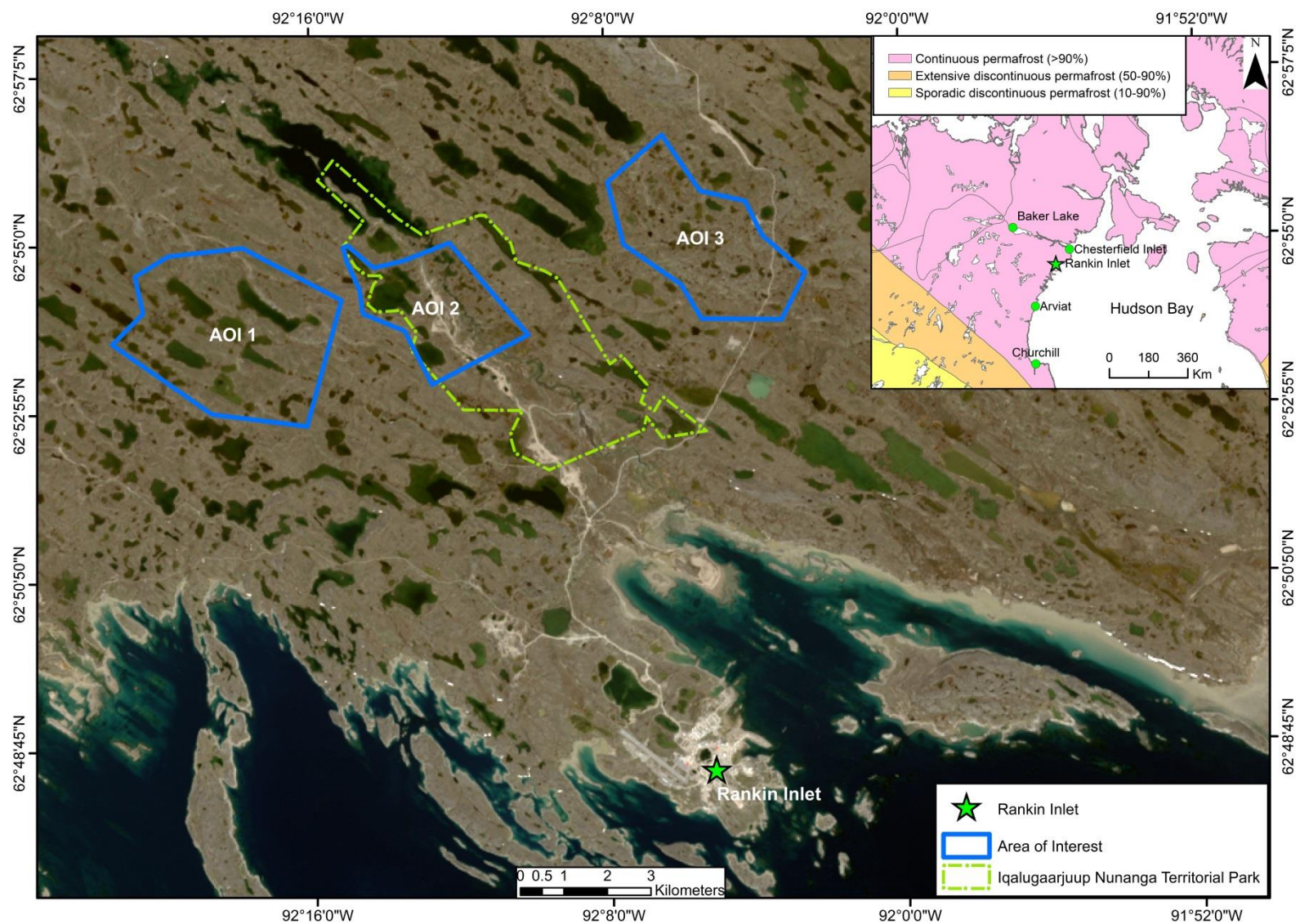


Figure 1: Study region near Rankin Inlet showing the three areas of interest (AOI) selected for lake analysis. Inset map shows Rankin Inlet on the coast of Hudson Bay in the continuous permafrost zone (after Heginbottom et al., 1995). Base map courtesy of the U.S. Geological Survey (United States Geological Survey, 2016)

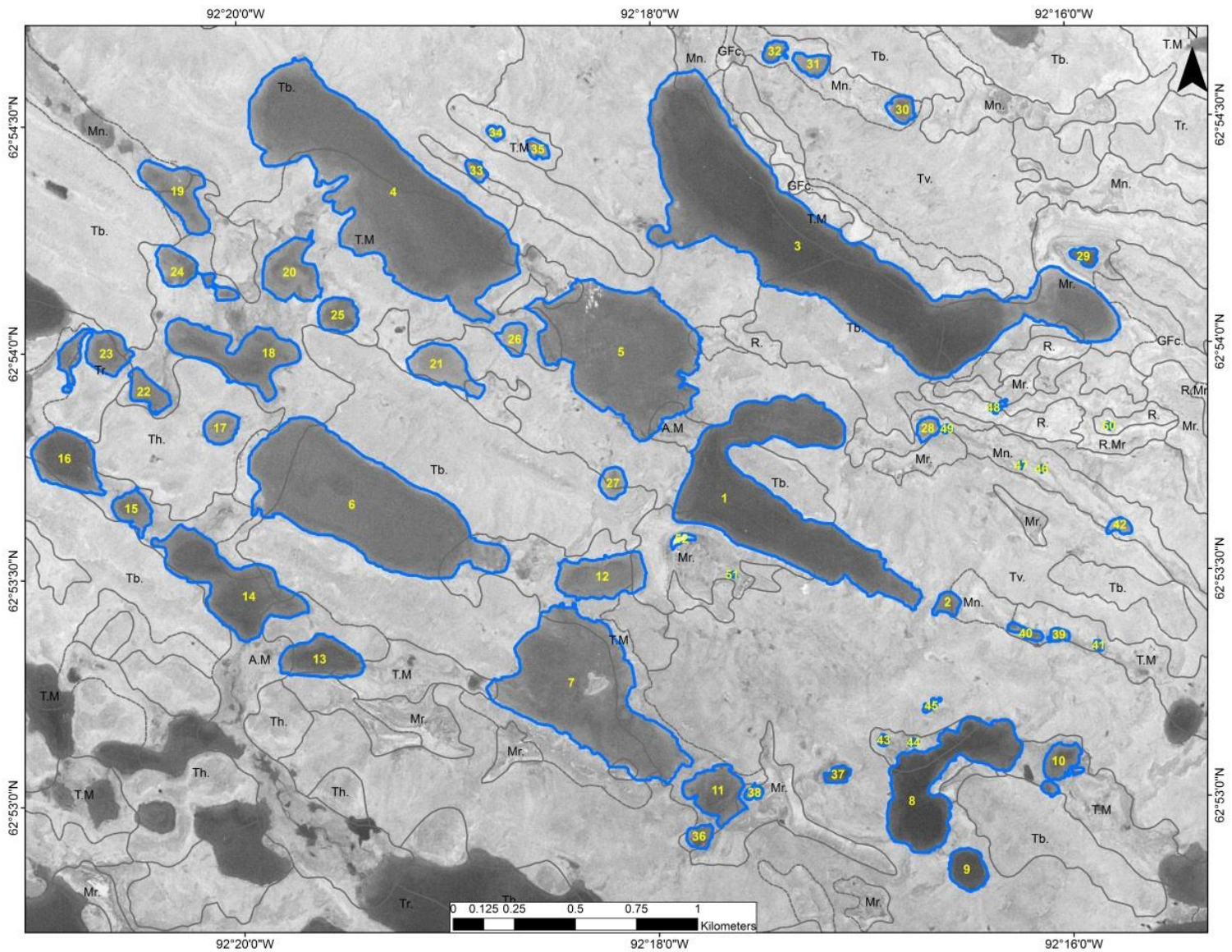


Figure 2: Area of interest 1 (AOI 1). Blue polygons depict lakes digitized for analysis. Grey polygons depict surficial geology (GSC, in press). Air photo 1954 (A14302_025). See Table 1 for surficial geology legend.

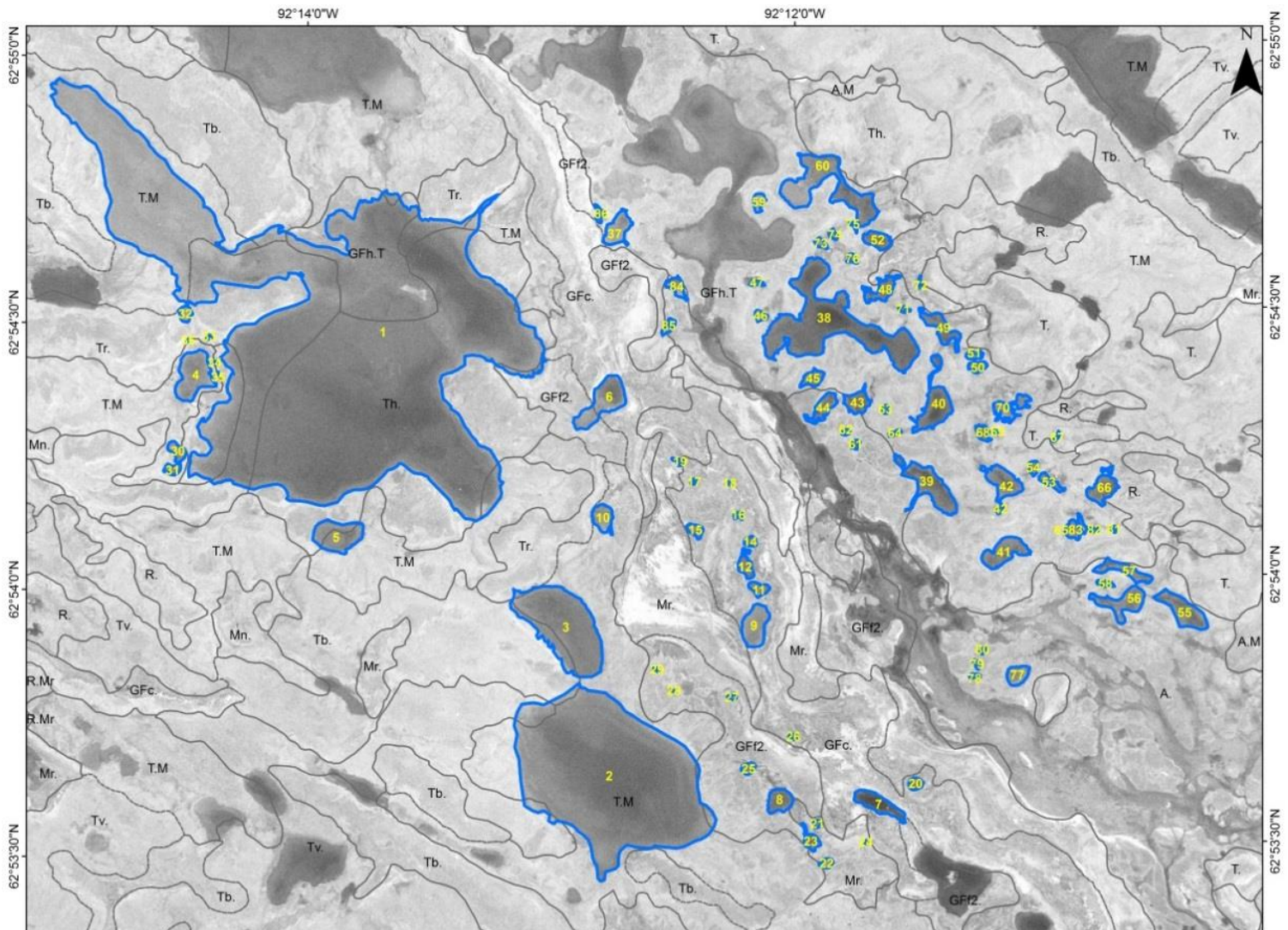


Figure 3: Area of interest 2 (AOI2). Blue polygons depict lakes digitized for analysis. Grey polygons depict surficial geology (GSC, in press). Air photo 1954 (A14302_026). See Table 1 for surficial geology legend.

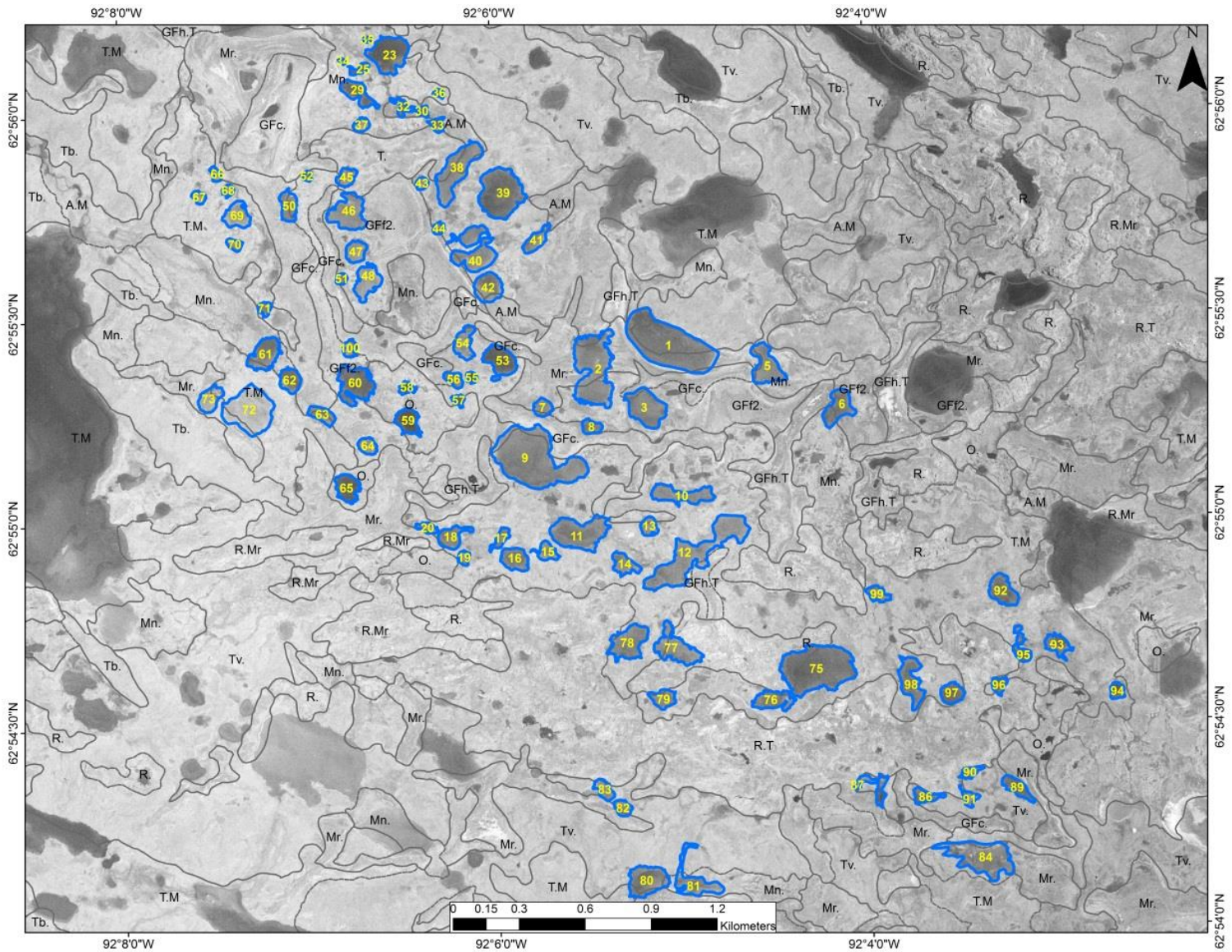


Figure 4: Area of interest 3 (AOI 3). Blue polygons depict lakes digitized for analysis. Grey polygons depict surficial geology (GSC, in press). Air photo 1954 (A14302_027). See Table 1 for surficial geology legend.

Table 1: Surficial geology unit abbreviation legend

Surficial Geology Units¹	Description¹
T	Till undifferentiated
T.M	Undifferentiated till and marine sediments
Tb	Till blanket
Tv	Till veneer
Tr	Ridged moraine
Th	Hummocky till
M	Marine sediments undifferentiated
Mr	Beach sediments
Md	Deltaic sediments
Mi	Intertidal sediments
Mn	Nearshore sediments
A	Alluvial sediments undifferentiated Undifferentiated alluvial and marine sediments
A.M	
GF	Glaciofluvial sediments
GF2	Subaqueous outwash fan sediments
GFh	Hummocky sediments
GFc	Ice-contact sediments
O	Organic
R	Bedrock undifferentiated
R2	Igneous bedrock, plutonic

1: Surficial geology units and description from Cocking et al. 2015

Table 2: Air photo information and orthorectification metadata

Air photo	Date	NTS map	Scale	Focal point (mm)	ΔX (mm)	ΔY (mm)	RMS X (m)	RMS Y (m)	RMS (m)
A14302_025	1954-07-14	055K16	1:50,000	153.19	105.769	105.728	0.1897	0.1683	0.1793
A14302_026	1954-07-15	055K16	1:50,000	153.19	105.769	105.728	0.1252	0.1481	0.1371
A14302_027	1954-07-16	055K16	1:50,000	153.19	105.769	105.728	0.1594	0.1521	0.1558
A14302_028	1954-07-17	055K16	1:50,000	153.19	105.769	105.728	0.1892	0.1285	0.1617
A17405_048	1961-08-02	055K16	1:60,000	152.56	105.708	105.686	0.1675	0.1913	0.1798
A17405_049	1961-08-03	055K16	1:60,000	152.56	105.708	105.686	0.1942	0.1132	0.1589
A18916_104	1965-07-11	055K16	1:90,000	88.11	105.941	105.926	0.1322	0.1141	0.1235
A18916_105	1965-07-12	055K16	1:90,000	88.11	105.941	105.926	0.1101	0.1258	0.1182
A21333_047	1969-08-25	055K16	1:15,000	305.38	118.072	118.235	0.719	0.7479	0.7336
A21333_048	1969-08-26	055K16	1:15,000	305.38	118.072	118.235	0.5786	0.5613	0.5700
A21333_049	1969-08-27	055K16	1:15,000	305.38	118.072	118.235	0.3541	0.4634	0.4124
A21333_105	1969-08-28	055K16	1:15,000	305.38	118.072	118.235	0.4013	0.6267	0.5262
A21333_106	1969-08-29	055K16	1:15,000	305.38	118.072	118.235	0.5116	0.4006	0.4595
A21333_108	1969-08-30	055K16	1:15,000	305.38	118.072	118.235	0.6174	0.3987	0.5197
A21333_109	1969-08-31	055K16	1:15,000	305.38	118.072	118.235	0.3844	0.5349	0.4658
A21333_113	1969-09-01	055K16	1:15,000	305.38	118.072	118.235	0.5971	0.3044	0.4739
A21333_114	1969-09-02	055K16	1:15,000	305.38	118.072	118.235	0.4301	0.5145	0.4742
A22951_027	1972-08-07	055K16	1:7,000	152.682	105.978	105.991	0.9819	1.1756	1.0831
A22951_028	1972-08-08	055K16	1:7,000	152.682	105.978	105.991	1.549	1.5667	1.5579
A22951_029	1972-08-09	055K16	1:7,000	152.682	105.978	105.991	1.6521	1.0321	1.3774
A24204_110	1975-07-15	055K16	1:25,000	153.26	106.013	105.982	0.4966	0.2668	0.3986
A24204_111	1975-07-16	055K16	1:25,000	153.26	106.013	105.982	0.2673	0.3876	0.3329
A24204_127	1975-07-17	055K16	1:25,000	153.26	106.013	105.982	0.6068	0.3522	0.4961
A24204_128	1975-07-18	055K16	1:25,000	153.26	106.013	105.982	0.3544	0.3926	0.3740
A24204_129	1975-07-19	055K16	1:25,000	153.26	106.013	105.982	0.4902	0.2254	0.3815
A24204_130	1975-07-20	055K16	1:25,000	153.26	106.013	105.982	0.4932	0.2519	0.3916
A24426_043	1976-07-29	055K16	1:20,000	153.264	105.984	105.994	0.5495	0.5924	0.5714
A24426_044	1976-07-30	055K16	1:20,000	153.264	105.984	105.994	0.5881	0.5053	0.5483
A26954_236	1976-07-31	055K16	1:20,000	153.027	105.979	105.997	0.3218	0.6234	0.4961
A26954_237	1986-07-09	055K16	1:20,000	153.027	105.979	105.997	0.3617	0.4946	0.4333
A26954_269	1986-07-10	055K16	1:20,000	153.027	105.979	105.997	0.4991	0.62	0.5628

A26954_270	1986-07-11	055K16	1:20,000	153.027	105.979	105.997	0.8889	0.5874	0.7534
Air photo	Date	NTS map	Scale	Focal point (mm)	ΔX (mm)	ΔY(mm)	RMS X (m)	RMS Y (m)	RMS (m)
A27836_091	1992-07-24	055K16	1:20,000	152.854	106	106.018	0.6085	0.7628	0.6900
A27836_092	1992-07-25	055K16	1:20,000	152.854	106	106.018	0.6042	0.461	0.5374
A27836_103	1992-07-26	055K16	1:20,000	152.854	106	106.018	0.5942	0.4457	0.5252
A27836_104	1992-07-27	055K16	1:20,000	152.854	106	106.018	0.5305	0.3939	0.4672
Average	N/A	N/A	N/A	N/A	N/A	N/A	0.5083	0.4675	0.4952

Table 3: Human error assessment analysis

Polygon	Area Operator 1 (m ²)	Area Operator 2 (m ²)	Area Operator 3 (m ²)	Absolute Difference Operator 1 vs 2 (m ²)	Absolute Difference Operator 1 vs 3 (m ²)	Absolute Difference Operator 2 vs 3 (m ²)	Average Difference between operators (m ²)	Average Difference between operators (%)
1	309359	310681	307060	1322	2298	3620	2414	0.78
2	7550	7665	7638	114	87	27	76	1.01
3	663950	662651	663567	1300	383	916	866	0.13
4	482353	484156	482805	1803	452	1352	1202	0.25
5	283719	280593	279909	3126	3810	684	2540	0.90
6	350076	341853	340578	8223	9499	1275	6332	1.81
7	284295	274315	272147	9979	12148	2168	8098	2.85
8	136612	137953	134418	1342	2194	3536	2357	1.73
9	20957	21061	20476	104	482	585	390	1.86
10	20718	16267	19395	4451	1323	3128	2967	14.32
11	39500	38181	40012	1319	512	1832	1221	3.09
12	53893	53206	53473	687	420	267	458	0.85
13	43703	43521	42970	182	733	551	488	1.12
14	121457	123062	121540	1605	82	1522	1070	0.88
15	18284	18354	16809	70	1476	1546	1031	5.64
16	52937	51129	50234	1808	2703	895	1802	3.40
17	14599	14310	14216	289	384	95	256	1.75
18	84300	84405	85020	104	719	615	479	0.57
19	44626	44809	44779	183	153	30	122	0.27
20	44152	44699	44662	547	510	37	365	0.83
21	37309	37308	37625	1	315	316	211	0.57
22	16943	16782	16688	160	255	95	170	1.00
23	37539	24168	24333	13371	13206	164	8914	23.75
24	26851	18878	18560	7973	8291	318	5527	20.59
25	19043	18835	18629	208	414	206	276	1.45
26	11707	11581	10999	126	708	582	472	4.03
27	10801	10181	10288	621	514	107	414	3.83
28	6540	6387	5961	153	579	426	386	5.90
29	5909	5070	5454	839	456	384	560	9.47
33	5259	5705	4847	445	412	857	572	10.87
34	3015	3249	3444	234	429	195	286	9.50
35	5357	4832	4673	525	684	159	456	8.51
36	7974	5253	7024	2721	950	1771	1814	22.75
37	5309	5147	5504	162	194	357	238	4.48
38	3074	2538	2346	536	728	192	485	15.79
39	3485	4213	3818	727	332	395	485	13.91

Polygon	Area Operator 1 (m ²)	Area Operator 2 (m ²)	Area Operator 3 (m ²)	Absolute Difference Operator 1 vs 2 (m ²)	Absolute Difference Operator 1 vs 3 (m ²)	Absolute Difference Operator 2 vs 3 (m ²)	Average Difference between operators (m ²)	Percentage of the average difference to total lake area (%)
40	4953	7601	4318	2648	635	3283	2189	44.19
41	1194	1274	1157	80	37	118	78	6.56
42	4756	3429	4703	1327	53	1274	885	18.60
43	1486	1372	1342	114	145	31	96	6.49
44	830	734	770	96	61	35	64	7.70
45	1986	1970	1299	15	687	672	458	23.06
46	527	556	630	29	103	74	69	13.02
47	393	573	463	181	70	111	121	30.73
48	1830	1023	1157	807	673	134	538	29.41
49	995	1169	1057	174	62	112	116	11.66
50	426	479	416	53	10	62	42	9.75
51	2871	2709	4107	162	1236	1398	932	32.47
Average	68863	67831	67569	1522	1513	802	1279	9.00

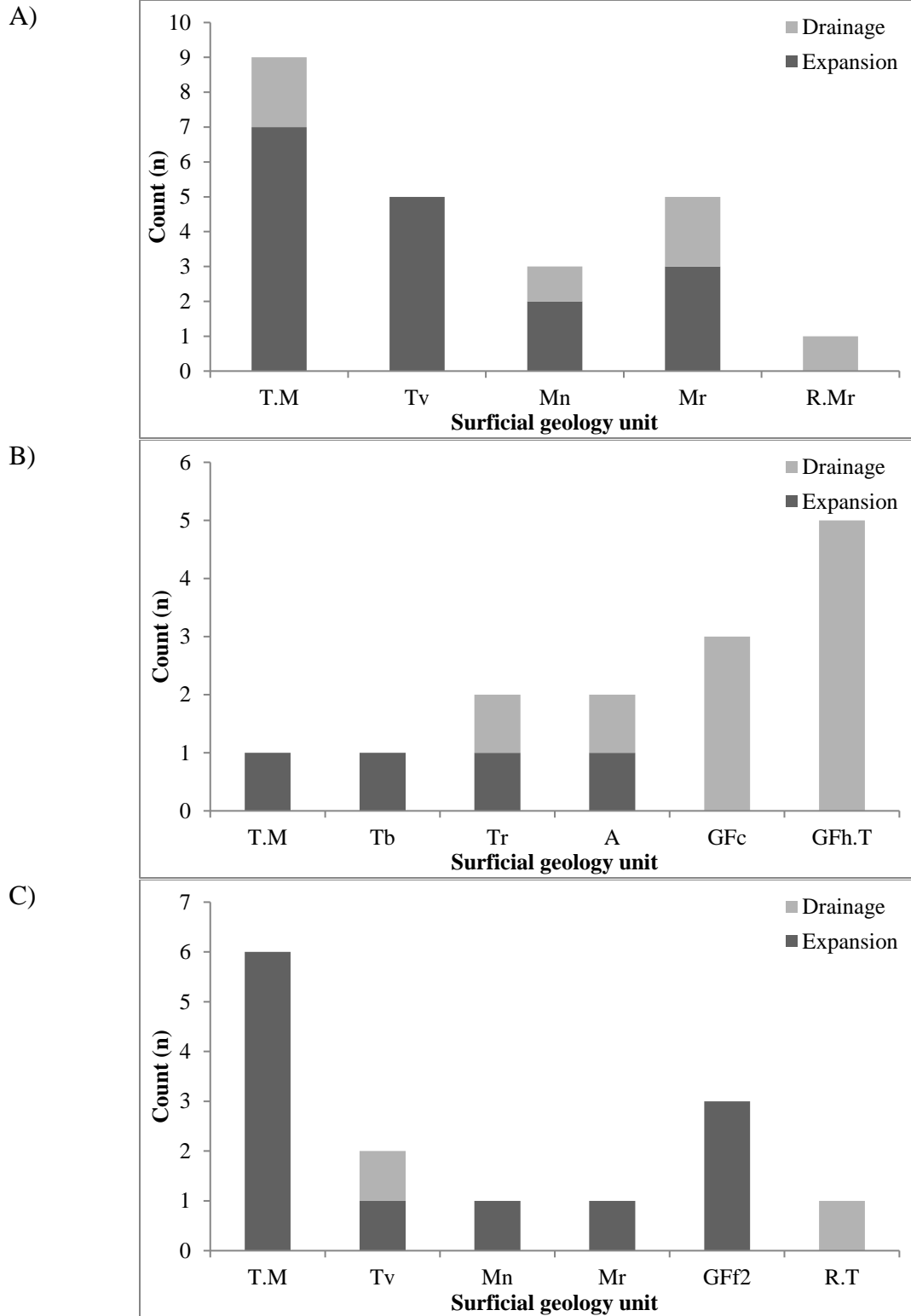


Figure 5 Distribution of surficial geology units associated with lake expansion or drainage for each AOI. A) AOI 1, B) AOI 2, C) AOI 3.